

AD-A054 398

SCIENCE APPLICATIONS INC WOODLAND HILLS CA
MIXING AND COMBUSTION IN HIGH SPEED AIR FLOWS. (U)
APR 78 R B EDELMAN, P T HARSHA F

F/G 21/2

UNCLASSIFIED

SAI-78-008-WH

AFOSR-TR-78-0878

F49620-77-C-0044

NL

1 OF 1
AD
A054398

END
DATE
FILMED
6-78

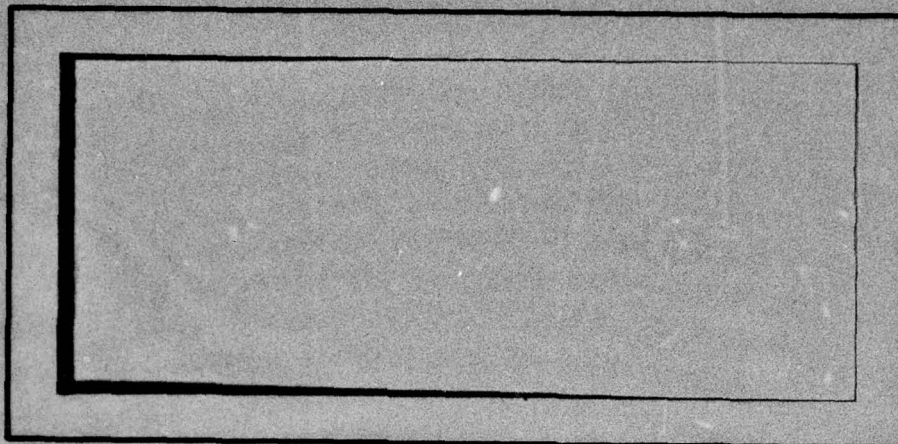
DDC

AFOSR-TR- 78-0878

FOR FURTHER TRAN

2

AD A 054398



SCIENCE APPLICATIONS, INC.

AD No. ~~1~~
C FILE COPY

See Form 1473

DDC
RECEIVED
MAY 26 1978
D

DISTRIBUTION STATEMENT A

Approved for public release;
Distribution Unlimited



AIR FORCE OFFICE OF SCIENTIFIC RESEARCH (AFOSR)
NOTICE OF TRANSMITTAL TO DDC
This technical report has been reviewed and is
approved for public release IAW AFR 190-12 (Vb).
Distribution is unlimited.
A. D. BLOSE
Technical Information Officer

ACCESSION for	
DTIC	White Section <input checked="" type="checkbox"/>
DDC	Buff Section <input type="checkbox"/>
UNANNOUNCED	<input type="checkbox"/>
JUSTIFICATION.....	
BY.....	
DISTRIBUTION/AVAILABILITY CODES	
Dist. AVAIL. and/or SPECIAL	
A	

✓ 
SAI-78-008-WH

**AFOSR INTERIM SCIENTIFIC REPORT:
MIXING AND COMBUSTION IN
HIGH SPEED AIR FLOWS**

AD A 054398

R. B. Edelman and P. T. Harsha

**Science Applications, Inc.
20335 Ventura Blvd., Suite 423
Woodland Hills, California 91364**

Prepared for

**Air Force Office of Scientific Research
Bolling Air Force Base
Washington, D.C. 20332**

F49620-77-C-0044
new

April 1978

AD No. 1
DDC FILE COPY

DDC
RECEIVED
MAY 26 1978
D

DISTRIBUTION STATEMENT A
Approved for public release;
Distribution Unlimited

916
393 451

SUMMARY

A modular model of the sudden-expansion combustor has been developed, combining a parabolic, directed-flow computation and a well-stirred reactor model representing the recirculation region(s). The parabolic module incorporates a turbulent kinetic energy turbulence model, and both modules use the quasi-global formulation for rapid computation of finite-rate chemical reactions. Coupling between the modules is through a shear layer representation which provides the parabolic-flow boundary conditions and the stirred-reactor feed rates. Compared to unified elliptic models of the dump combustor, the major advantage of this approach is the greatly increased detail possible in the combustor analysis. This detail in turn allows the development of chemical kinetic and flowfield models applicable to the refinement of elliptic formulations. The modular concept is currently being applied in ramjet performance analysis under an AFAPL program and in combustor models emphasizing alternate fuels under DoE support.

ABSTRACT

This report describes the development of a modular model for the prediction of the performance of sudden expansion burners as a function of the controllable parameters relevant to combustor design. The model is based upon a concept in which the recirculation zone, treated as a stirred reactor, is coupled to a parabolic boundary layer formulation for the flow outside the recirculation zone. Hydrocarbon oxidation kinetics and turbulent kinetic energy models are employed in the model development. In addition to the parabolic-flow and stirred reactor elements, a module representing the fuel injection process has been developed. Results of the application of the modular model to the analysis of cold-flow and reacting-flow dump combustor experimental data are described.

TABLE OF CONTENTS

I.	INTRODUCTION	1
II.	MODULAR MODEL CONCEPT	3
III.	MODULAR MODEL FORMULATION	6
	1. Coupling Relations: The Shear Layer Model	6
	2. Well-Stirred Reactor: The Recirculation Zone Model	9
	3. Parabolic Mixing: The Directed-Flow Model	12
	4. Chemical Kinetics: The Quasi-Global Model	18
IV.	MODELS FOR THE FUEL INJECTION PROCESS	21
V.	RESULTS OF APPLICATION OF THE MODULAR MODEL	24
VI.	FURTHER WORK	33
VII.	REFERENCES	35

LIST OF FIGURES

FIGURE	PAGE
1. Schematic of Sudden Expansion (Dump) Burner	4
2. Coupling Relation Definition Sketch	7
3. Predicted Fuel Mass Fraction Distributions For Simultaneous Injection at Three Radial Locations. Inlet Air Velocity 700 ft/sec, Inlet Air Temperature 1600 °K, Overall Equivalence Ratio 0.6.	23
4. Schematic of Tested and Predicted Flow Configuration Cold Flow	25
5. Sensitivity of Computed Wall Static Pressure Distributions to Dividing Streamline Shape and Shear Stress Assumptions	27
6. Comparison of Computed and Experimental Centerline Mach Number Profiles, Cold Flow Case	28
7. Schematic of Tested and Predicted Flow Configuration Reacting Flow	30
8. Representative Calculation Result Reacting Flow Case	31

LIST OF TABLES

TABLE	PAGE
1. Extended C-H-O Chemical Kinetic Reaction Mechanism $k_f = AT^b \exp(-E/RT)$	20

NOMENCLATURE

<u>SYMBOL</u>	<u>MEANING</u>	<u>EQUATION</u>
a	constant in shear layer width expression	1
a_1	parameter in shear stress - turbulent energy relationship	22
a_2	turbulent kinetic energy dissipation constant	21
b	{ constant in shear layer width expression characteristic width of mixing region	1 19
c	eddy viscosity constant	19
h	static enthalpy	17
H	total enthalpy	16,17
k	turbulent kinetic energy	20
l	characteristic length scale	1
l_k	turbulent kinetic energy dissipation length scale	21
\dot{m}	stirred reactor mass flow rate	5
M_i	molecular weight species i	12,18
p_c	pressure	15,18
P_r	turbulent Prandtl number	16
Pr_k	turbulent Prandtl number for kinetic energy	21
\dot{Q}	heat inflow to stirred reactor	6,10
r	radial coordinate	3
R	universal gas constant	12,18
R_c	radius of dividing streamline between directed flow and recirculation region	10,11
R_T	turbulent Reynolds number	25
S_c	turbulent Schmidt number	16

NOMENCLATURE (cont.)

<u>SYMBOL</u>	<u>MEANING</u>	<u>EQUATION</u>
T	temperature	12,18
u	axial mean velocity component	13
U_c	axial mean velocity component on centerline	23
U_j	axial mean velocity component on centerline at $X/D = 0$	23
u'	axial turbulent velocity component	20
v	radial mean velocity component	13
V	stirred reactor volume	7
v'	radial turbulent velocity component	20
w'	azimuthal turbulent velocity component	20
\dot{W}_i	chemical production term for species i	11,14
\dot{W}_k^G	production of k th gas specie due to homogeneous gas phase reactions	7
\dot{W}_k^P	production of k th particle class	7
x	axial coordinate	13
y	lateral coordinate in parabolic mixing model	13
α_i	mass fraction of species i	7,14
ϵ_D	eddy kinematic viscosity	10,11
ϵ_m	eddy kinematic viscosity at half- velocity point	25
ϵ_v	gas phase eddy viscosity	14
κ	gas thermal conductivity	10
μ_T	turbulent dynamic viscosity, $= \rho \epsilon_v$	19

NOMENCLATURE (Cont.)

<u>SYMBOL</u>	<u>MEANING</u>	<u>EQUATION</u>
ρ	density	12
ρ_c	characteristic density of recirculation region	10,11
τ_T	shear stress	22
ψ	stream function	-

SUBSCRIPTS

$()_i$	species i
P	outside dividing streamline
R	inside dividing streamline
w	dividing streamline

SUPERSCRIPTS

$()^I$	influx to stirred reactor
$()^O$	outflow from stirred reactor

I. INTRODUCTION

Current and future airbreathing propulsion system concepts are tending toward lower weight and smaller volume designs. An example is the integral rocket/ramjet engine which uses a common combustor for rocket boost and sustained ramjet flight. Unfortunately, the current design trends create stringent requirements for higher performance from smaller volumes, and the combustion processes are not well enough understood so that combustor development has been carried out largely by employing costly cut-and-try methods.

The basic difficulty in understanding combustor behavior is the coupling between turbulent mixing and reaction kinetics. This problem is not unique to combustor flows, but is encountered in other systems where flow, mixing, and reaction times are all of the same order of magnitude, for example, external burning devices for thrust and/or control and in gas dynamic and chemical laser systems. In addition, many of the reacting flows of general interest involve condensed phase species and large scale recirculation zones such as are found in the "dump" burner concept. Problems in ignition, flame stabilization, combustion efficiency, and flowfield and combustion instabilities also occur in the dump burner as well as in many other combustion systems of interest, and these problems need to be better understood to support engineering judgement.

Consequently, continued research is required in both subsonic and supersonic flows in order to gain the necessary understanding of the controlling mechanisms. Only in this way can effective design principles be developed to provide optimum propulsion system performance over wide operating ranges.

The objective of the work summarized in this report is to eliminate the deficiencies just described and provide a sound basis for effective combustor design criteria, through the

development of analytical models for the sudden-expansion combustor flowfield. The major emphasis in this program is on the development of a "modular" model for the sudden expansion combustor, in which proved computational elements, including a parabolic flowfield analysis procedure and a perfectly-stirred reactor formulation are coupled together to model the overall flowfield. In this report the features of the modular approach are reported and progress in the development and application of the model to cold-flow and reacting-flow combustor data is described. This work has involved, and will continue to involve, close coordination with the experimental work in progress at the Air Force Aero Propulsion Laboratories at Wright-Patterson Air Force Base, as well as other related programs.

II. MODULAR MODEL CONCEPT

The basic characteristics of the sudden expansion burner are depicted in Figure 1. In essence, the key feature of the flow field is the recirculation region just downstream of the expansion, separated from the directed flow by the dividing streamline. Because of this recirculation region, in which there is no characteristic flow direction, the flow field in the sudden expansion burner is in general described by elliptic equations; i.e., the boundary layer approximations cannot be applied to the whole flow and the elliptic Navier-Stokes equations must be used. However, it is possible, at least conceptually, to divide the flow field into two regions. The first, the directed flow region, consists of that part of the flow between the dividing streamline and the burner centerline. The second region is the recirculating flow region, and the two regions are coupled through the conditions at the dividing streamline.

The concept of the modular approach to the computation of the flow in a sudden expansion burner involves the application of available techniques to the separate regions of the flow field. Thus, the directed flow region is treated using a parabolic finite difference solution of the boundary layer form of the equations of motion. The recirculation regions are treated as perfectly stirred reactors, with the reactor feed rate defined by the species diffusion flux across the dividing streamline. The shape of the dividing streamline must be specified a priori; the resulting wall static pressure distribution may then be compared with experiment and another dividing streamline shape specified, if necessary. Since the flow field is in general elliptic, the modular approach approximates the true flow field, and the specification of the species fluxes across the dividing streamline must be carried out iteratively. However, despite

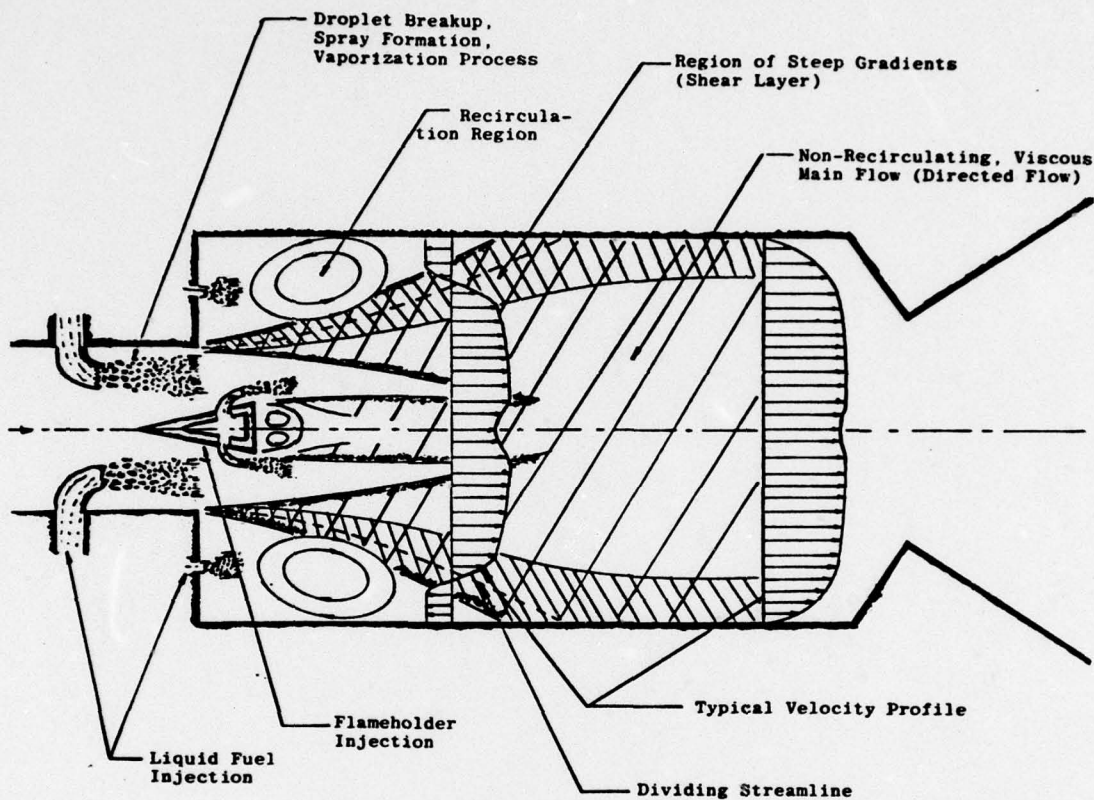


Figure 1. Schematic of Sudden Expansion (Dump) Burner

April 1978

SAI-78-008-WH

its limitations, this method does allow the application of well-tested and proved flow models to the sudden expansion burner geometry, and is capable of yielding parametric information of interest in sudden expansion burner design.

III. MODULAR MODEL FORMULATION

The basic elements of the current modular model formulation are the parabolic finite-difference computational technique developed by Boccio, Weilerstein and Edelman [1], modified to incorporate the turbulent kinetic energy model developed by Harsha [2], used for the directed-flow portion of the analysis, and the stirred reactor computation developed by Edelman and Weilerstein [3]. Both of these elements make use of the quasi-global model developed by Edelman and Fortune [4] for rapid computation of finite-rate hydrocarbon air kinetics. These elements, or modules, are coupled together through a simplified representation of the turbulent shear layer which exists between the directed flow and the recirculation region. In the modular approach, the shear layer representation is used to define the gradients in velocity, species, and enthalpy between the two regions of the flow, thus providing both the boundary conditions on the directed flow and the stirred reactor feed rates. Details of the mathematical formulations used for the flowfield region are discussed in this section; details of the numerical analysis procedure may be found in Ref. [5].

1. Coupling Relations: The Shear Layer Model

The key feature of the modular concept lies in the coupling relations assumed along the dividing streamline that (1) supply the boundary condition for the parabolic computations and (2) determine the feed rates for the perfectly stirred reactor computation. These coupling conditions are obtained through a simplified model of the turbulent shear layer separating the recirculation zone from the directed flow, as is shown schematically in Figure 2. Note in the following that the shear layer is assumed to be vanishingly thin, that is, the gradients established through the shear layer model are applied along the

dividing streamline.

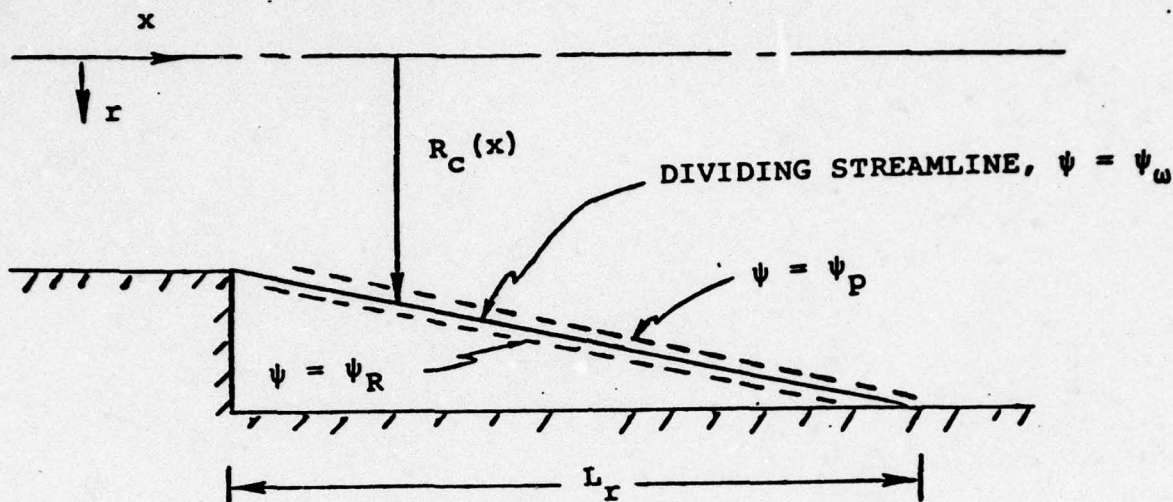


Figure 2. Coupling Relation Definition Sketch

It is assumed that the shear layer can be modeled as a region of width $l(x)$ across which all dependent variables (i.e., velocity, temperature, turbulent kinetic energy, and species mass fractions) vary linearly. The width of the shear layer is itself assumed to be specifiable by the relation

$$l = a + bx \quad (1)$$

in which a and b are constants. Since, for planar shear layers, the growth rate can be related to the dividing streamline shear stress, specification of the constant b implies a shear stress distribution along the dividing streamline, while the constant a can be taken to be a parameter which is related to the boundary layer thickness at the step.

As shown in Figure 2, the dividing streamline shape, $R_c(x)$ is specified; this specification also defines the dividing

streamline stream function value $\psi = \psi_w$. Along ψ_w , the turbulent shear stress τ_w is defined as described above, and thus the turbulent kinetic energy k_w is defined through the relation

$$\tau_w = 0.3 \rho k_w \quad (2)$$

To obtain the gradients in temperature and species mass fraction, linear profiles across the shear layer are assumed. If ψ_p is defined as the streamline immediately "outside" the recirculation region (i.e., within the directed flow) and ψ_R is the streamline immediately "inside" the recirculation zone, then, for species i

$$\left. \frac{\partial \alpha_i}{\partial r} \right|_w = \frac{\alpha_{ip} - \alpha_{iR}}{\ell} \quad (3)$$

and for the temperature

$$\left. \frac{\partial T}{\partial r} \right|_w = \frac{T_p - T_R}{\ell} \quad (4)$$

where α_{ip} and T_R are the values of species mass fractions and temperature obtained from the stirred reactor solution.

The overall flowfield computation using the modular approach proceeds as follows. A dividing streamline shape $R_c(x)$ is assumed, and the shear layer width expression and shear stress distribution is defined. An initial state for the stirred reactor computation is assumed, resulting in values of α_{iR} and T_R . With these data available as boundary conditions, the parabolic mixing calculation is carried out to the end of the recirculation zone. This calculation defines the species mass fraction and temperature gradients at $\psi = \psi_w$, and these values are used to obtain the stirred reactor feed rates. A new stirred reactor computation is carried out using the new feed rates, resulting in a new specification of α_{iR} and T_R , and the parabolic computation is repeated. The procedure is repeated until the changes in the stirred reactor composition from computation to computation become small, at

which point the coupling iteration has converged. The parabolic calculation is then carried out to the end of the combustion chamber, completing the solution.

2. Well-Stirred Reactor: The Recirculation Zone Model

Flowfield regions in which intense backmixing occurs can approach the limit of complete mixing, and thus the well-stirred reactor concept is attractive for representing the recirculation region in the sudden expansion burner. Because the mixing process is considered to be complete, the mathematical formulation for the perfectly stirred reactor is straightforward. The describing equations are given as follows:

Global Conservation of Mass:

$$\dot{m} = \text{constant} - \sum_k \dot{m}_k^I = \sum_k \dot{m}_k^O \quad (5)$$

where k is the k^{th} component which can include i gas-phase species and j droplet types. A droplet type (or class) is defined by its composition (fuel, water, etc.) and its size. The superscripts I and O refer to inflow and outflow, respectively.

Conservation of Energy:

$$h = h^I + \dot{Q}/\dot{m} \quad (6)$$

where \dot{Q} is the net rate of external heat addition to the zone and the inflow of enthalpy is written to allow each component to enter the reactor with an arbitrary temperature.

Conservation of Species:

The conservation of species k requires that its net outflow be equal to the rate of production due to chemical and phase transition processes. Formally, this principle gives k equations of the form:

$$\alpha_k = \alpha_k^I + \frac{V}{\dot{m}} \left(\dot{W}_k^G + \dot{W}_k^P \right) \quad (7)$$

where superscripts G and P refer to homogeneous gas-phase and dropwise production rates, respectively.

Although there exist more or less standard techniques for the solution of such algebraic equations, an alternative approach involves the use of the non-steady form of the species conservation equations, viz:

$$\frac{d\alpha_k}{dt} = \frac{m}{\rho V} (\alpha_k^I - \alpha_k) + \left(\frac{\dot{W}_k}{\rho}\right)^G + \left(\frac{\dot{W}_k}{\rho}\right)^P \quad (8)$$

where t is the time variable of significance only during the transient period. Thus, Equation (8) is identical to Equation (7) when:

$$\frac{d\alpha_k}{dt} \rightarrow 0 \quad (9)$$

The remaining working equations retain their steady state form.

These equations, along with expressions for the volumetric production rates appearing in equation (8), expressions for the enthalpy as a function of species concentrations and the equation of state, define the temperature and species concentrations in the stirred reactor, given the inflow rates for species and enthalpy. In the modular model, the net inflow of species and enthalpy can be expressed as line integrals involving gradients evaluated along the dividing streamline, so that for the modular model the energy and species conservation equations for the stirred reactor can be written

ENERGY

$$\begin{aligned} -2\pi \int_0^S R_C(x) \rho \epsilon_D \sum_i \left[h_i^I(T^I) \frac{\partial \alpha_i^I}{\partial r} \right] ds + \dot{Q} - 2\pi \int_0^S R_C(x) \kappa \frac{\partial T}{\partial s} ds = \\ = 2\pi \int_0^S R_C(x) \rho \epsilon_D \sum_i \left[h_i^O(T_R) \frac{\partial \alpha_i^O}{\partial r} \right] ds \end{aligned} \quad (10)$$

SPECIES

$$\frac{d\alpha_i}{dt} = \frac{-2\pi}{\rho_c V} \int_0^s R_C(x) \left[\rho \epsilon_D \frac{\partial \alpha_i^I}{\partial r} \right] ds - \frac{2\pi}{\rho_c V} \int_0^s R_C(x) \left[\rho \epsilon_D \frac{\partial \alpha_i^O}{\partial r} \right] ds + \frac{\dot{W}_i}{\rho_c} \quad (11)$$

neglecting the dropwise species production rate term. Here the superscript I refers to inflow into the stirred reactor (recirculation region) and superscript o refers to outflow from the stirred reactor, V is the reactor volume, ρ_c a characteristic density of the stirred reactor region, and $\rho \epsilon_D$ a characteristic eddy diffusivity, evaluated from the outer flow field solution in the region of the dividing streamline. The term \dot{W}_i represents the rate of production of species i caused by chemical reactions and \dot{Q} represents the heat input to the stirred reactor region through the combustor walls.

Equations (10) and (11), along with an equation of state

$$\rho = \frac{P}{RT \sum_i \frac{\alpha_i}{M_i}} \quad (12)$$

where

R = the universal gas constant

M_i = the molecular weight of species i

are used to establish a new reactor state, given the feed rates established from the parabolic directed flow solution; i.e., given the diffusive fluxes of species and energy across the dividing streamline, Equations (10), (11) and (12) are solved for new values of the α_i and the recirculation zone temperature, T_R . The process is then iterated until changes in the para-

meters describing the state of the recirculation zone are small.

3. Parabolic Mixing: The Directed-Flow Model

The next major element of the modular model for a sudden expansion combustor is the formulation for the directed flow portion of the combustor flowfield. It is assumed that the boundary layer approximations apply to this part of the flowfield, so that the describing equations are parabolic. For a steady, axisymmetric flow these equations may be written:

Global Continuity

$$\frac{\partial y \rho u}{\partial x} + \frac{\partial y \rho v}{\partial y} = 0 \quad (13)$$

Species Diffusion for the i^{th} Specie:

$$\rho u \frac{\partial \alpha_i}{\partial x} + \rho v \frac{\partial \alpha_i}{\partial y} = \frac{1}{y} \frac{\partial}{\partial y} \left\{ y \rho \frac{\epsilon_v}{S_c} \left[\frac{\partial \alpha_i}{\partial y} \right] \right\} + \dot{w}_i \quad (14)$$

Momentum Equation:

$$\rho u \frac{\partial u}{\partial x} + \rho v \frac{\partial u}{\partial y} = \frac{1}{y} \left\{ \frac{\partial}{\partial y} \left(y \rho \epsilon_v \frac{\partial u}{\partial y} \right) \right\} - \frac{\partial p}{\partial x} \quad (15)$$

and the energy equation

$$\begin{aligned} \rho u \frac{\partial H}{\partial x} + \rho v \frac{\partial H}{\partial y} = \frac{1}{y} \frac{\partial}{\partial y} \left\{ \frac{y \rho \epsilon_v}{P_r} \left[\frac{\partial H}{\partial y} - \left(\frac{P_r}{S_c} - 1 \right) \right. \right. \\ \left. \left. \sum_i h_i \frac{\partial \alpha_i}{\partial y} + (P_r - 1) \frac{\partial}{\partial y} \left(\frac{u^2}{2} \right) \right] \right\} \end{aligned} \quad (16)$$

in which P_r and S_c represent the Prandtl and Schmidt numbers, respectively. These equations, along with expressions for the

enthalpy

$$\left. \begin{aligned} H &= h + u^2/2 \\ h &= \sum_i \alpha_i h_i(T) \end{aligned} \right\} \quad (17)$$

and the equation of state

$$p = \rho RT \sum_i (\alpha_i / M_i) \quad (18)$$

can be solved, given an expression for the turbulent momentum diffusivity ϵ_v , or the turbulent eddy viscosity $\mu_T = \rho \epsilon_v$. The problem of the most appropriate formulation for the eddy viscosity in a turbulent flow has occupied the attention of researchers in turbulent flow for many years, and numerous proposals for the appropriate form of the eddy viscosity have been made. In general, up until a few years ago, models for the turbulent eddy viscosity involved a relation between a local length scale and a local measure of the velocity gradient. The free turbulent mixing model proposed by Prandtl in 1942 [6] is a case in point; with this model

$$\mu_T = \rho c b |\Delta u| \quad (19)$$

where c is a constant, b is a measure of the width of the mixing region, and Δu a measure of the velocity difference across the mixing region.

While eddy viscosity models have in certain circumstances enabled successful calculations of particular turbulent flows to be carried out, in general, the constant of proportionality involved in the model varies markedly and unpredictably in different flow fields [7].

The observed lack of generality of eddy viscosity models has led to the development of a class of models in which additional partial differential equations are written to obtain

the spatial variation of the turbulent shear stress. Of these, the most highly developed are the turbulent kinetic energy models (8, 9).

If the turbulent kinetic energy is defined as

$$k = 1/2 (\bar{u}'^2 + \bar{v}'^2 + \bar{w}'^2) \quad (20)$$

an equation describing the spatial variation of this quantity can be obtained from the momentum and continuity equations by appropriate manipulations.

For steady axisymmetric compressible flow the turbulent kinetic energy equation can be written [2]

$$\underbrace{\rho u \frac{\partial k}{\partial x} + \rho v \frac{\partial k}{\partial y}}_I = \underbrace{\frac{1}{y} \frac{\partial}{\partial y} \left(\frac{y \mu_T}{Pr_k} \frac{\partial k}{\partial y} \right)}_{II} + \underbrace{\mu_T \left(\frac{\partial u}{\partial y} \right)^2}_{III} - \underbrace{\frac{a_2 \rho k^{3/2}}{l_k}}_{IV} \quad (21)$$

in which the various terms are interpreted as:

- I transport by mean flow (advection)
- II diffusion
- III production
- IV dissipation

In order to use Equation (21), a relationship between the turbulent shear stress, τ , and the turbulent kinetic energy, k , must be postulated. One such relationship is

$$\tau_T = a_1 \rho k \quad (22)$$

For most turbulent shear flows the parameter a_1 must be allowed to vary laterally. In general, for an axisymmetric jet or ducted flow, a_1 can be written [2]

for $U_c > 0.9 U_j$

$$a_1 = 0.3 \left(\frac{\partial u}{\partial y} \right) / \left| \frac{\partial u}{\partial y} \right| \quad (23)$$

for $U_c \leq 0.9 U_j$ and $y < y_{\max}$

$$a_1 = 0.3 \left(\frac{\partial u}{\partial y} \right) / \left| \frac{\partial u}{\partial y} \right|_{\max} \quad (24)$$

for $U_c \leq 0.9 U_j$ and $y \geq y_{\max}$

$$a_1 = 0.3 \left(\frac{\partial u}{\partial y} \right) / \left| \frac{\partial u}{\partial y} \right|$$

where U_c represents the local axial velocity component on the centerline, U_j the value of the centerline velocity at the jet origin, y_{\max} the value of y at which $\left| \frac{\partial u}{\partial y} \right|$ is a maximum, and $\left| \frac{\partial u}{\partial y} \right|_{\max}$ the maximum value of $\left| \frac{\partial u}{\partial y} \right|$. Further details regarding the lateral variation of a_1 may be found in Reference 2.

To describe the variation of a_2 , which appears in the dissipation term of Equation (21), a "turbulent Reynolds number" defined by

$$R_T = \frac{\Delta u l_k}{\epsilon_m} \quad (25)$$

is used as the independent variable. This parameter is a function of x only. The term ϵ_m represents the eddy kinematic viscosity at the maximum shear point in a lateral profile, i.e.,

$$\epsilon_m = (\tau_m / \rho_m) / (\partial u / \partial y)_m \quad (26)$$

and l_k is a characteristic length scale, effectively the lateral width of the turbulent flow. This scale, which is also used in the dissipation expression Equation (21), is determined by the

following set of relationships.

For the two-dimensional shear layer, or first regime of a jet (i.e., for $U_c = U_j$)

$$l_k = \Delta y \quad (27)$$

where Δy is the lateral distance between the points at which $(u-u_e)/(u_j-u_e) = 0.95$ and $(u-u_e)/(u_j-u_e) = 0.05$, for profiles which are not fully developed. In these expressions, u_e is the velocity at the outer edge of a jet; at a wall $u_e = 0$. For fully developed profiles, which can be approximated by a cosine function,

$$l_k = 1.57 \Delta u / (\partial u / \partial y)_m \quad (28)$$

where the subscript m again refers to the position in a lateral profile at which the shear stress is a maximum. Equation (28) provides a characteristic length scale determination which avoids the problem of defining the edge of an asymptotic profile. Because the cosine function is not always a good approximation to the true computed velocity profile, in practice Equation (28) is only used in place of Equation (27) wherever the value of l_k determined by it satisfies the inequality $\Delta y \leq l_k \leq 1.57 \Delta y$.

For the second regime of jets, i.e., when

$$u_c < u_j$$

$$l_k = 2r_{1/2} \quad (29)$$

where $r_{1/2}$ is the value of r at which $(u-u_e)/(u_c-u_e) = 0.5$.

In the definition of R_T , $\Delta u = u_j - u_e$ in the first regime of jets, and $\Delta u = u_c - u_e$ in the second regime of jets.

The value of the dissipation constant, a_2 , is related to the local value of R_T and to the initial jet density ratio.

These relationships were obtained through comparison of prediction with a wide variety of jet and wake experiments [2]; in summary, they are:

Variation in a_2 with R_T

$$\begin{aligned} \text{for } 0 < R_T \leq 185, & \quad a_2 = 1.69 \\ \text{for } 185 < R_T \leq 360, & \quad a_2 = 0.46 + 0.00762R_T \\ \text{for } R_T > 360, & \quad a_2 = 3.20 \end{aligned} \quad (30)$$

Variation in a_2 with density ratio

For nonunity initial density ratio, multiply a_2 by $1/c_1$, where, for

$$\frac{\rho_{e1}}{\rho_{j1}} > 1 \quad c_1 = 0.984 + 0.016 \frac{\rho_{e1}}{\rho_{j1}} \quad (31)$$

and for

$$\frac{\rho_{e1}}{\rho_{j1}} < 1 \quad c_1 = 0.95 + 0.05 \left(R_{eT_{Te}} \right) / \left(R_{jT_{Tj}} \right) \quad (32)$$

In these relations, the subscript 1 refers to conditions at the origin of mixing, R_e is the gas constant appropriate to the outer flow, and T_{Te} is the total temperature of that flow. Equation (32) is used when the jet density is greater than the free-stream density in order to preserve the a_2 - R_T relationship for the supersonic shear-layer case, for which the "jet" side is taken to be the high-speed stream. Thus, for the case of compressible but identical-gas mixing problems, the value of c_1 obtained through use of Equation (32) is unity, while for gases with different molecular weights or stagnation temperatures a nonunity c_1 is obtained.

The turbulent kinetic energy model described in this section has been successfully applied to a wide variety of flows, with and without variation in density. For free flows, numerous examples of the applications of this model are given in Reference 2; it has also been applied recently to the computation of ducted flows [10].

The complete set of describing equations for the parabolic flowfield is thus made up of equations (13) - (18) along with equation (21) and its associated algebraic relations. With boundary conditions prescribed from the stirred reactor solution through use of the coupling conditions described in Section III.1, these equations are numerically integrated using the solution technique of Reference [1] as described in detail in Reference [5].

4. Chemical Kinetics: The Quasi-Global Model

In both the stirred reactor and directed flow portions of the modular model the volumetric production rate terms appearing in the species transport equations are evaluated using a full hydrocarbon chemical kinetics scheme based on the quasi-global kinetics model [4]. This model has as a key element a subglobal

oxidation step



This reaction is unidirectional with an empirically determined rate (grams of fuel/cc/sec) given by

$$A T^b P^{0.3} [C_n H_m]^{\frac{1}{2}} [O_2] \exp[-(E/RT)] \quad (34)$$

with the constants A, b, and E/R defined in Table 1, where P must be given in atmospheres, T in degrees Kelvin and [] denotes molar concentration.

Coupled to this subglobal step are the intermediate reversible reactions given in Table 1. Some observations on this scheme should be noted. First, it is generally agreed that in hydrogen bearing systems carbon monoxide is most rapidly oxidized to CO₂ via the reaction



We have, however, included other reactions involving CO and oxygen for completeness including



and



where M is the general third body. Reactions (36) and (37) are much slower than reaction (35), but their inclusion was necessary for basic studies performed on systems including the CO/air system. In addition, a number of reactions involving NO_x are included which represent a necessary extension of the basic Zeldovich mechanism to account for certain of the ambient long time NO-to-NO₂ conversion reactions which occur in the atmosphere particularly when coupled with appropriate daylight photochemical mechanisms.

Table 1. Extended C-H-O chemical kinetic reaction mechanism $k_f = AT^b \exp(-E/RT)$

Reaction	A Long Chain Cyclic		Forward b	E/R Long Chain Cyclic	
1) $C_nH_{2n+2}O_2 \rightarrow \frac{n}{2}H_2 + n CO$	6.0×10^4	2.08×10^7	1	12.2×10^3	19.65×10^3
2) $CO + OH = H + CO_2$	5.6×10^{11}		0	$.543 \times 10^3$	
3) $CO + O_2 = CO_2 + O$	3×10^{12}		0	25.0×10^3	
4) $CO + O + M = CO_2 + M$	1.8×10^{19}		-1	2×10^3	
5) $H_2 + O_2 = OH + OH$	1.7×10^{13}		0	24.7×10^3	
6) $OH + H_2 = H_2O + H$	2.19×10^{13}		0	2.59×10^3	
7) $OH + OH = O + H_2O$	5.75×10^{12}		0	$.393 \times 10^3$	
8) $O + H_2 = H + OH$	1.74×10^{13}		0	4.75×10^3	
9) $H + O_2 = O + OH$	2.24×10^{14}		0	8.45×10^3	
10) $M + O + H = OH + M$	1×10^{16}		0	0	
11) $M + O + O = O_2 + M$	9.38×10^{14}		0	0	
12) $M + H + H = H_2 + M$	5×10^{15}		0	0	
13) $M + H + OH = H_2O + M$	1×10^{17}		0	0	
14) $O + H_2 = H + HO$	1.36×10^{14}		0	3.775×10^4	
15) $H_2 + O_2 = H + NO_2$	2.7×10^{14}		-1.0	6.06×10^4	
16) $H_2 + O_2 = NO + HO$	9.1×10^{24}		-2.5	6.46×10^4	
17) $NO + NO = H + NO_2$	1.0×10^{10}		0	4.43×10^4	
18) $NO + O = O_2 + H$	1.55×10^9		1.0	1.945×10^4	
19) $M + NO = O + H + M$	2.27×10^{17}		-0.5	7.49×10^4	
20) $M + NO_2 = O + NO + M$	1.1×10^{16}		0	3.30×10^4	
21) $M + NO_2 = O_2 + H + M$	6.0×10^{14}		-1.5	5.26×10^4	
22) $NO + O_2 = NO_2 + O$	1×10^{12}		0	2.29×10^4	
23) $H + OH = NO + H$	4×10^{13}		0	0	
24) $H + NO_2 = NO + OH$	3×10^{13}		0	0	
25) $CO_2 + H = CO + HO$	2×10^{11}		-1/2	4×10^3	
26) $CO + NO_2 = CO_2 + NO$	2×10^{11}		-1/2	2.5×10^3	

$$^a \frac{dC_{C_nH_{2n+2}O_2}}{dt} = -A T^b P^{0.3} C_{C_nH_{2n+2}O_2} C_{O_2} \exp\left(-\frac{E}{RT}\right); [C] = \frac{\text{moles}}{\text{cc}}, [T] = ^\circ K, [P] = \text{atm}, [E] = \frac{\text{k cal}}{\text{mole}}$$

Reverse reaction rate k_r is obtained from k_f and the equilibrium constant K_c .

IV. MODELS FOR THE FUEL INJECTION PROCESS

In addition to the basic components of a parabolic, directed flow analysis and a well-stirred reactor formulation, the modular concept can be extended to include modules which represent other elements of the dump combustor flowfield, for example, the fuel injection process. The detail of the computation provided by the use of a parabolic directed flow analysis (as opposed to the relative coarseness of the numerical grid allowable in current unified, elliptic solution techniques) is the key feature of the modular model that allows the inclusion of a fuel injection module in the complete analysis. This is particularly true in the case of liquid fuel injection, for at the fuel/air ratios appropriate for dump combustor operation, the liquid fuel streams initially occupy a very small portion of the overall combustor cross-sectional area. It is also worth noting that it has been stated that the further development of unified, elliptic combustor flowfield calculations requires the development of what are essentially modular models for such features as the fuel injection process (Reference 11) since these key processes occur on scales much smaller than feasible numerical resolution allows. Thus the development of fuel injection, vaporization, and spreading models through use of the overall modular model concept is necessary for further development of unified techniques.

The liquid fuel injection model makes use of a combination of empirical information and turbulent mixing calculations. For example, the fuel jet penetration from the wall is computed through the use of the penetration correlation developed by Catton, Hill and McRae (Ref. 12), using the breakup time correlation developed by Clark (Ref. 13) to compute the downstream distance at which penetration is to be computed. That is, it is assumed that the fuel jet has turned parallel to the airflow

at the axial position at which the initial fuel jet has broken up into droplets, as given by the breakup time correlation and the local airflow velocity.

Since the basic modular model formulation involves an axisymmetric flowfield, individual fuel jets cannot be resolved, and it is assumed in the formulation that the liquid fuel spray forms an annulus whose cross-sectional area may either be specified or computed based on an assumed fuel spray bulk velocity. A bulk spray evaporation correlation is then used to compute the fuel vaporization rate; this correlation, developed by Ingebo and Foster [14] is a function of the initial velocity and temperature difference between the fuel spray and the surrounding air stream. Spreading of the fuel jet is computed through use of a turbulent mixing hypothesis as for the mixing process in the remainder of the parabolic flow.

Figure 3 shows the results of a computation of the fuel injection process for three fuel injectors, located in the combustor inlet wall, along the centerline, and in a midstream position. Shown are the computed contours of the fuel mass fraction, α_F , with the vapor-phase fuel shown as the solid line and the liquid phase fuel as the dotted line, as a function of both axial and radial position in the combustor inlet. For these calculations the air inlet velocity was approximately 700 ft/sec at a temperature of 1600 °K; the overall fuel-air equivalence ratio was 0.6. The results shown in Figure 3 provide a good example of the detail of the fuel injection process available through use of this aspect of modular modeling.

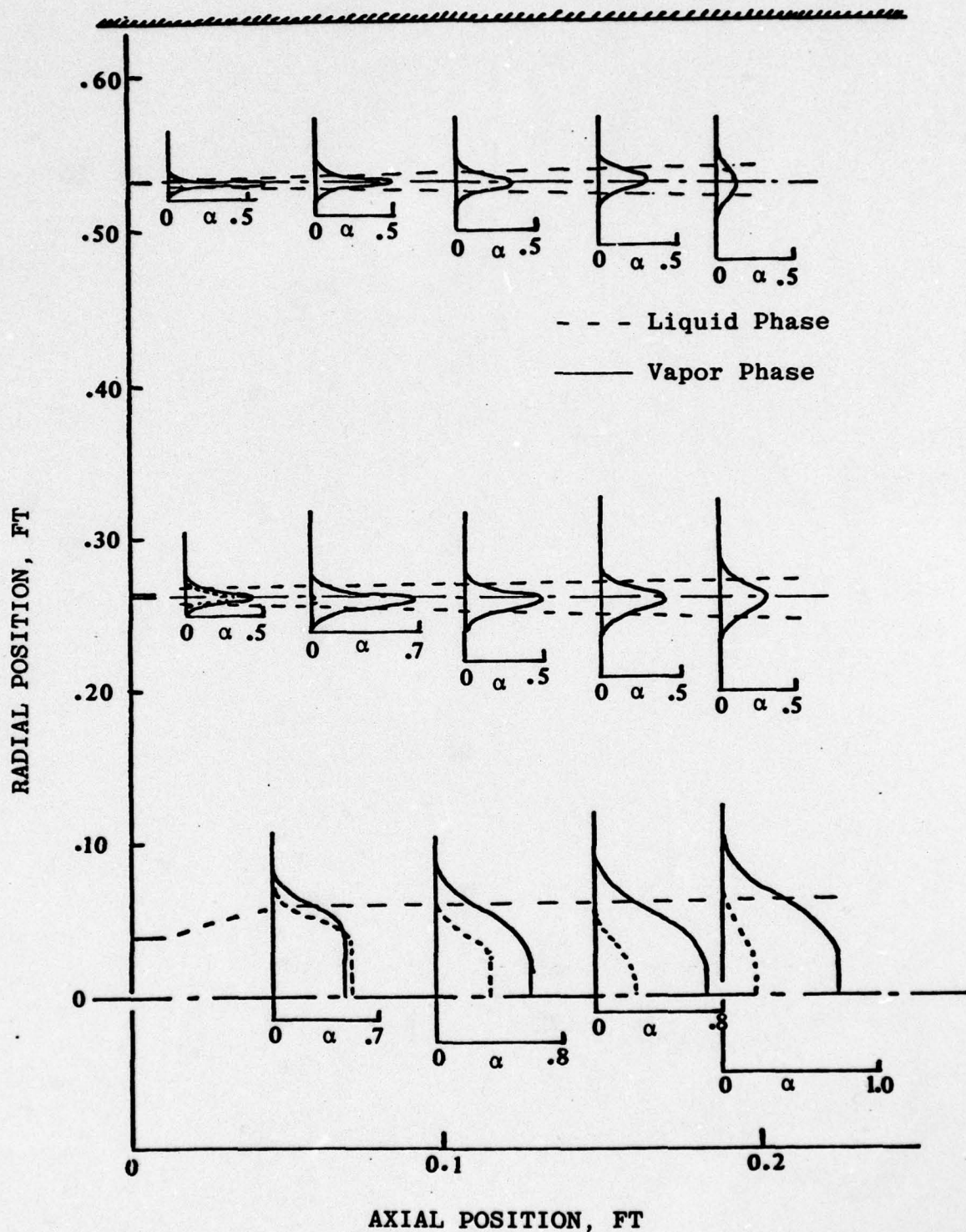


Figure 3. Predicted Fuel Mass Fraction Distributions for Simultaneous Injection at Three Radial Location. Inlet Air Velocity 700 ft/sec, Inlet Air Temperature 1600 °K, Overall Equivalence Ratio 0.6.

V. RESULTS OF APPLICATION OF THE MODULAR MODEL

During this contract period, development work on the modular dump combustor analysis has centered on combining the elements of the analysis and determining the sensitivity of the results obtained using the approach to the assumptions involved in the model. The basic accuracy of the directed flow module, incorporating a finite-rate kinetics mechanism and the one-equation TKE turbulence model, was earlier tested in a series of computations of a reacting hydrogen-air jet, as reported in Ref. 15.

In order to test the predictions of the modular approach, a series of calculations were carried out for comparison with the cold-flow experimental results obtained by Drewry (Ref. 16). The configuration tested in these experiments is shown schematically in Figure 4, which also gives the initial conditions for the experiment and the computations. Note that the length of the recirculation zone used in the calculation is that measured by Drewry, as shown in Figure 4.

The sensitivity of the computed wall static pressure profile to the assumptions made in the model about the shape of the dividing streamline and the dividing streamline shear stress distribution is shown in Figure 4. Initially, the dividing streamline was assumed to have a linear shape, and a shear stress level typical of a pipe flow was chosen. The shear stress is represented on Figure 4 as a skin friction coefficient, where

$$C_f = \tau_{d.s.l.} / \left(\frac{1}{2} \rho_{c.l.} U_{c.l.}^2 \right)$$

for ease in comparison of the shear stress levels with values appropriate for ducted flows. It can be seen that the pipe-flow value of C_f produces a considerably larger static pressure rise than is experimentally observed, and that the assumption

AR INJECTION; $\dot{m}/\dot{m}_a = 0.03$

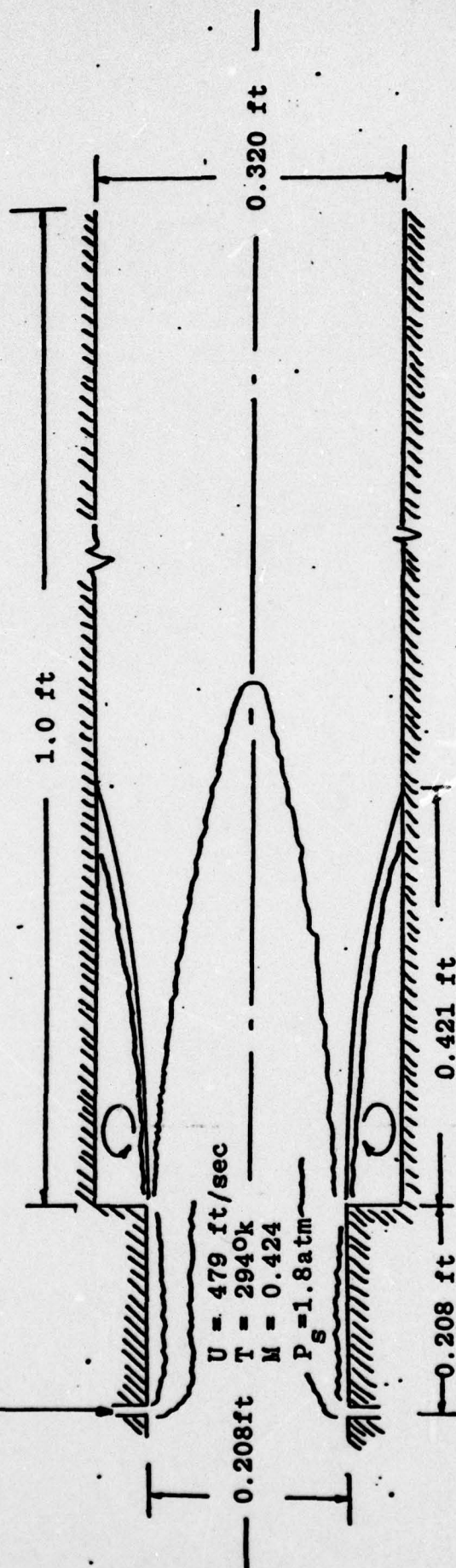


Figure 4. SCHEMATIC OF TESTED AND PREDICTED FLOW CONFIGURATION - COLD FLOW

of a linear shape produces a too rapid rate of increase of pressure. Thus, the shape of the dividing streamline was changed to a parabola, such that the overall length of the recirculation region was unchanged and the dividing streamline was initially parallel to the combustor wall at the dump station. As can be seen from Fig. 5, this produced a more gentle initial rate of pressure rise, although, with the same C_f , the ultimate pressure achieved was of course the same.

As can be seen from Fig. 5, the combination of a parabolic dividing streamline shape and a value of $C_f=0.060$ produced a computed static pressure profile in good agreement with the experiment. It should be noted, that if a Prandtl eddy viscosity model is considered for the shear layer region, a value of $C_f=0.060$ is equivalent to a Prandtl model constant of 0.018, which is in good agreement with the values reported for shear layer analyses.

Figure 6 shows a comparison between the computed and measured centerline Mach number profiles for the same cold flow case; it is clear from these results that somewhat too rapid mixing is predicted in the directed flow. Study of the results indicates that the problem may lie in the modeling of the turbulent length scale distribution. The dump burner flow is realistically a two-scale problem, with one turbulent length scale related to the turbulent shear layer region and a second scale more appropriate for the directed flow. Thus for these flow-fields, a two-equation turbulence model, in which the length scale distribution is computed through a transport equation as part of the solution may be more appropriate and will be incorporated in future work.

Computations for a representative reacting dump burner flow have also been carried out, again in order to assess the sensitivity of the results obtained to the assumptions used in the model. A schematic of the configuration involved is shown

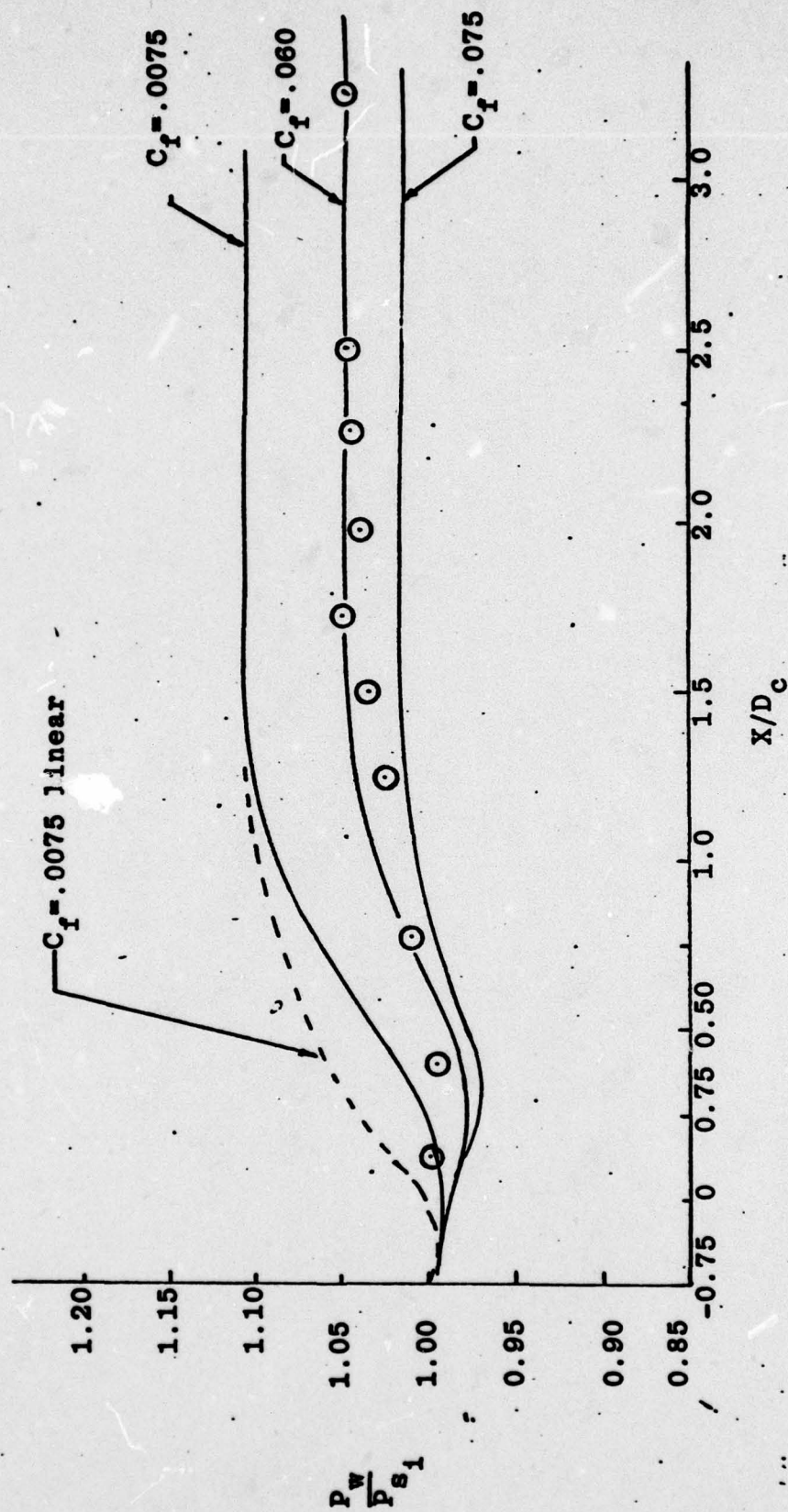


Figure 5. SENSITIVITY OF COMPUTED WALL STATIC PRESSURE DISTRIBUTIONS TO DIVIDING STREAMLINE SHAPE AND SHEAR STRESS ASSUMPTIONS

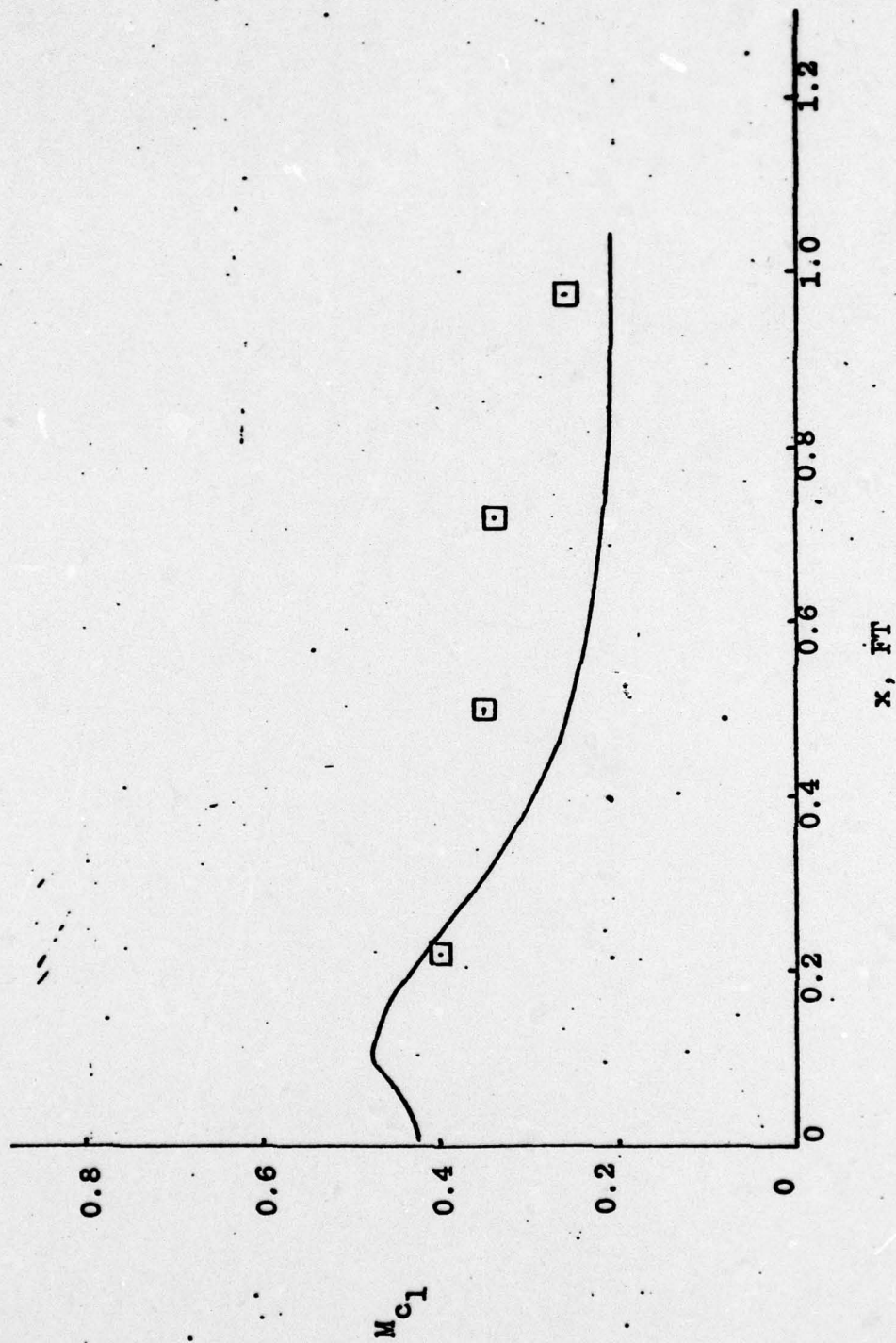


Figure 6. COMPARISON OF COMPUTED AND EXPERIMENTAL
CENTERLINE MACH NUMBER PROFILES, COLD FLOW CASE

in Figure 7, which also gives the conditions for the computations. The stirred reactor was assumed to contain the products of a fully-reacted, equilibrium, stoichiometric hydrocarbon-air combustion process; the temperature of the resulting mixture was arbitrarily specified. In order to perform preliminary computations very rapidly, a global finite-rate combustion model was used in the directed flow. The recirculation zone geometry was assumed to be the same as was used in the cold flow calculations.

Figure 8 shows that results of a representative computation of a hot flow case; here a 2200K recirculation zone temperature has been assumed. The cross-hatching indicates the region in which significant combustion is occurring in the directed flow. One important observation made from a series of such computations such as that shown here is the importance of the assumed initial shear layer thickness (i.e., the inlet boundary layer thickness) and the assumed shear layer growth rate. The expression for the shear layer growth rate is $l=a+bx$, where l is the shear layer width scale; a and b are shown on the figure. Increasing the initial thickness and growth rate of the shear layer reduces the rate of transfer through the shear layer and thus reduces the temperature rise in the directed flow delaying the onset of combustion. On the other hand, if the assumed shear stress level on the dividing streamline is increased (as in general is required for an increase in shear layer growth rate) the rate of momentum and energy transport is increased, and the increased residence time caused by the resultant retardation of the main flow allows more combustion to take place.

All of the effects mentioned above manifest themselves quite strongly in the computed axial static pressure gradient, so that this parameter can apparently be a tentative indicator of some of the details of the combustion process occurring within the dump burner.

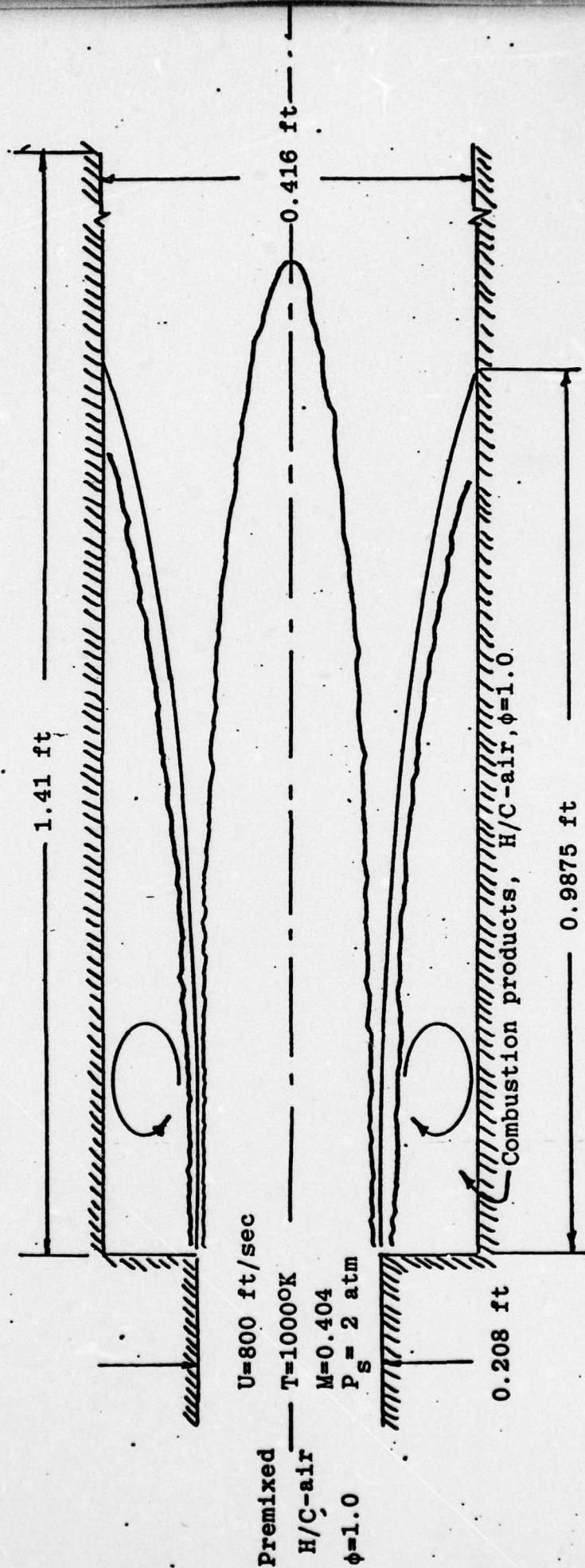


Figure 7. SCHEMATIC OF TESTED AND PREDICTED FLOW CONFIGURATION - REACTING FLOW

$a = 0.017$
 $b = 0.05$
 $c_f = 0.008$

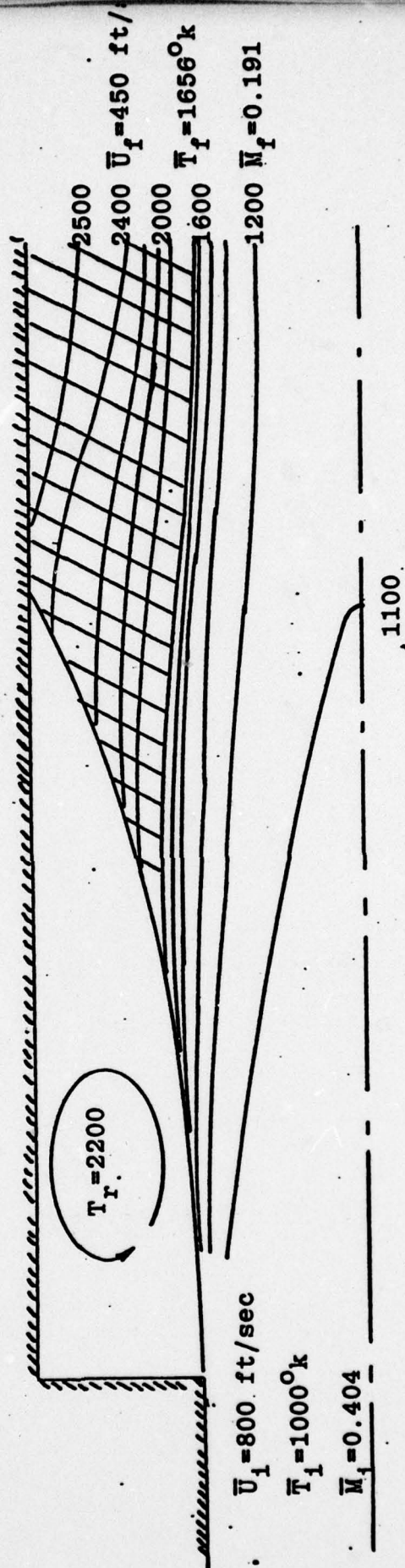


Figure 8. REPRESENTATIVE CALCULATION RESULT
 REACTING FLOW CASE

April 1978

SAI-78-008-WH

In addition to the progress achieved in the application of the model described above, during the current contract period close coordination has been maintained with Drs. F. D. Stull and J. E. Drewry at AFAPL. This has included providing a critical review of the designs for experimental hardware currently under test at AFAPL, and further recommendations for appropriate instrumentation for both hot-and cold flow testing based on the results of use of the modular model.

VI. FURTHER WORK

Work on the development and exploitation of the modular combustor model will continue, with emphasis on the inclusion of advanced turbulence models to adequately assess the effects of the different turbulence scales in different parts of the flow, as described in the preceding section, and on the inclusion of the effects of swirl in the directed portion of the flow.

Exploitation of the modular model will involve the use of the tool to develop a family of experiments relevant to hydrocarbon fuel injection and combustion, emphasizing the effects of different fuels including methane, ethylene and the higher hydrocarbons, and alternate fuels derived from non-petroleum sources. The focus of this work will be on the generation of a data base on steady-state combustion performance and flame stabilization in sudden expansion burners.

The modular model will also be used to obtain a preliminary assessment of the effects of turbulence levels, initial boundary layer thickness, and initial turbulence scale distribution on combustor performance. The effects of the degree of fuel vaporization at the combustor entrance and within the recirculation zones will also be assessed. These results will be used in examining existing data and identifying important new data required for model verification and refinement. In addition, aid will be provided toward the design of test configurations and instrumentation (including probe design) based on the resources available at AFAPL.

Further, a number of recent investigations of the use of unified models in combustor flowfields have pointed out the need for modular modeling within an overall elliptic formulation to overcome the grid resolution problems commonly encountered in the development of unified codes for reacting flowfields. Thus the development of a unified model specifically designed for the sudden-expansion combustor geometry which incorporates

April 1978

SAI-78-008-WH

modular features represents a natural development and extension of our current model formulation.

Finally, work done to date indicates that additional detail is required in modeling the fuel injection and vaporization process. Thus, modular model computations will be utilized to develop a more detailed characterization of the fuel spray process.

VII. REFERENCES

1. Boccio, J. L., Weilerstein, G., and Edelman, R. B., "A Mathematical Model for Jet Engine Combustor Pollutant Emissions," NASA CR-12108, GASL TR-781, General Applied Science Laboratories.
2. Harsha, P. T., "A General Analysis of Free Turbulent Mixing," AEDC TR-73-177, Arnold Engineering Development Center, 1974.
3. Edelman, R. B., and Weilerstein, G., unpublished work, 1971.
4. Edelman, R. B. and Fortune, O., A Quasi-global Chemical Kinetic Model for the Finite Rate Combustion of Hydrocarbon Fuels, AIAA Paper 69-86, 1969.
5. Edelman, R. B. and Harsha, P. T., "AFOSR Interim Report on Mixing and Combustion in High Speed Air Flows," RDA-TR-0700-002, April 1976.
6. Prandtl, L., "Bemerkungen zur Theorie der Freien Turbulenz," Zeitschrift fur Angewandte Mathematik und Mechanik, Vol. 22, 1942, pp. 241-243.
7. Harsha, P. T., Free Turbulent Mixing: A Critical Evaluation of Theory and Experiment, Arnold Engineering Development Center, AEDC TR-71-36, 1971.
8. Harsha, P. T., "Kinetic Energy Methods," Chapter 8 of Handbook of Turbulence, Vol. 1, W. Frost and T. Moulden, Eds., Plenum Publishing Corp., 1977.
9. Launder, B. E. and Spalding, D. B., Lectures in Mathematical Models of Turbulence, Academic Press, 1972.

10. Harsha, P. T. and Glassman, H. N., "Analysis of Turbulent Unseparated Flow in Subsonic Diffusers," Journal of Fluids Engineering, Vol. 98, No. 2, June 1976, pp. 320-322.
11. Abou Ellail, M. M., Gosman, A. D., Lockwood, F. C., and Megahed, I. E. A., "Description and Validation of Three-Dimensional Procedure for Combustion Chamber Flows," To Be Published in Journal of Energy.
12. Catton, I., Hill, D. E. and McRae, R. D., "Study of Liquid Jet Penetration in a Hypersonic Stream," AIAA Journal, Vol. 6, No. 11, November 1977.
13. Clark, B., "Break-up of a Liquid Jet in a Transverse Flow of Gas," NASA TN-D-2424, August 1964.
14. Ingebo, R. and Foster, H., "Drop Size Distribution for Cross-Current Break-up of Liquid Jets in Air Stream," NASA TN-4087, October 1957.
15. Edelman, R. B., and Harsha, P. T., "Some Observations on Turbulent Mixing with Chemical Reactions," AIAA Paper 77-142, January 1977.
16. Drewry, James E., "Characterization of Sudden-Expansion Dump Combustor Flowfields," AFAPL-TR-76-52, Air Force Aero Propulsion Laboratory, July 1976.

UNCLASSIFIED

SECURITY CLASSIFICATION OF THIS PAGE (When Data Entered)

1. REPORT DOCUMENTATION PAGE		READ INSTRUCTIONS BEFORE COMPLETING FORM	
18. REPORT NUMBER AFOSR TR-78-0878	2. GOVT ACCESSION NO.	3. RECIPIENT'S CATALOG NUMBER	
4. TITLE (and Subtitle) MIXING AND COMBUSTION IN HIGH SPEED AIR FLOWS		5. TYPE OF REPORT & PERIOD COVERED INTERIM rept. 1 Dec 76 - 31 Mar 78	
6. AUTHOR(s) R. B. EDELMAN P. T. HARSHA		7. PERFORMING ORG. REPORT NUMBER SAI-78-008-WH	
9. PERFORMING ORGANIZATION NAME AND ADDRESS SCIENCE APPLICATIONS, INC 20335 VENTURA BLVD, SUITE 423 WOODLAND HILLS, CA 91364		8. CONTRACT OR GRANT NUMBER(s) F49620-77-C-0044	
11. CONTROLLING OFFICE NAME AND ADDRESS AIR FORCE OFFICE OF SCIENTIFIC RESEARCH/NA BLDG 410 BOLLING AIR FORCE BASE, D C 20332		10. PROGRAM ELEMENT, PROJECT, TASK AREA & WORK UNIT NUMBERS 2308A2 61102F	
14. MONITORING AGENCY NAME & ADDRESS (if different from Controlling Office)		12. REPORT DATE 11 Apr 78	
		13. NUMBER OF PAGES 44	
		15. SECURITY CLASS. (of this report) UNCLASSIFIED	
		15a. DECLASSIFICATION/DOWNGRADING SCHEDULE 12/46P	
16. DISTRIBUTION STATEMENT (of this Report) Approved for public release; distribution unlimited.			
17. DISTRIBUTION STATEMENT (of the abstract entered in Block 20, if different from Report)			
18. SUPPLEMENTARY NOTES			
19. KEY WORDS (Continue on reverse side if necessary and identify by block number) SUDDEN EXPANSION (DUMP) BURNER INTEGRAL ROCKET/RAMJET ENGINE RECIRCULATING REACTING HIGH-SPEED FLOWS MODELING SUDDEN-EXPANSION COMBUSTOR FLOWFIELD			
20. ABSTRACT (Continue on reverse side if necessary and identify by block number) This report describes the development of a modular model for the prediction of the performance of sudden expansion burners as a function of the controllable parameters relevant to combustors design. The model is based upon a concept in which the recirculation zone, treated as a stirred reactor, is coupled to a parabolic boundary layer formulation for the flow outside the recirculation zone. Hydrocarbon oxidation kinetics and turbulent kinetic energy models are employed in the model development. In addition to the parabolic-flow and stirred reactor elements, a module representing the fuel injection process has been developed. Results of the application of the modular model to the analysis of cold-flow and reacting-flow dump combustor experimental data are described.			

DD FORM 1 JAN 73 1473 EDITION OF 1 NOV 65 IS OBSOLETE

UNCLASSIFIED

SECURITY CLASSIFICATION OF THIS PAGE (When Data Entered)

393 051